Diffraction measurements for evaluating plastic strain in A533B ferritic steela feasibility study

S J Lewis, C E Truman

Diffraction measurements for evaluating plastic strain in A533B ferritic steel – a feasibility study

S. J. Lewis and C. E. Truman

Department of Mechanical Engineering
University of Bristol
Bristol, U.K.

May 13, 2010

Abstract

It is known that the physical properties of many engineering materials may be strongly affected by previous loading, in particular prior plastic deformation. Most obviously, work hardening will alter subsequent yielding behaviour. Plastic deformation may also preferentially align the material microstructure, resulting in anisotropy of subsequent behaviour and a change in material fracture resistance.

When physical characterisation is undertaken by experimental testing it is, therefore, important to have some knowledge of the current state of the material. As a result, it is desirable to have methods of quantitatively evaluating the level of plastic deformation which specimen material may have experienced prior to testing.

This paper presents the results of a feasibility study, using a ferritic reactor pressure vessel steel, into the use of diffractive methods for plastic strain evaluation. Using neutron diffraction, changes in diffraction peak width and anisotropy of peak response were correlated with plastic deformation in a tensile test. The relationships produced were then used to evaluate permanent deformation levels in large samples, representative of standard fracture toughness test specimens.

1 Introduction

Failure of engineering components, such that they are no longer able to fulfil their designed function, is generally deemed to occur by one of two criteria. The first of these is excessive deformation, due to overload and resulting yielding. The second broad class of failure is fracture; propagation of a crack through a component such that the stiffness is degraded or the component is split into two or more pieces. Yielding behaviour in the majority of engineering materials is well characterised,

such that failure by excessive deformation can be relatively accurately predicted. Prediction of fracture behaviour is considerably less reliable, due largely to the fact that the macroscopic phenomenon of crack propagation and fracture may be caused by a number of competing micro-mechanical processes.

Ductile fracture results from growth and coalescence of voids within a material. Initially, the increasing void volume fraction is balanced by strain hardening behaviour increasing local yield stress. However, there comes a point where the reduction in load bearing area can no longer be maintained and failure occurs. In the case of brittle fracture micro-cracks, often nucleated at material inclusions or defects, are propagated by high levels of local matrix stress along preferred crystallographic planes [1] or along grain boundaries.

Both mechanisms are deemed to be controlled by local stresses, in general maximum principal stress for cleavage and inter-granular fracture [2, 3] and local hydrostatic stress for ductile fracture [4]. The effect of residual stress fields, due to prior loading or manufacturing processes, on fracture behaviour is well documented [5, 6] and the measurement of residual stress in components by diffraction, e.g. [7], and strain relaxation methods [8, 9] is well established.

There is an increasing body of evidence [10, 11], however, highlighting the effect of plastic strain history on ensuing fracture behaviour. The level of plastic strain is often assumed to control nucleation of micro-cracks in brittle fracture [12] and the degree of void growth in ductile failure [13]. As such, in order to accurately predict fracture behaviour, it is important to have accurate knowledge of the plastic strain history as well as the stress levels in the component.

Methods of stress measurement by material removal and measurement of resultant strain relaxation are inherently based on assumptions of elastic stress-strain behaviour and therefore offer no insight into determination of plastic strain levels. Therefore, it is necessary to use methods based on phenomena at the scale of the material grain structure and atomic lattice, such as those based on diffraction.

Plastic strain history has previously been investigated using a number of methods including x-ray diffraction [14] and electron back scatter diffraction [15] but from an engineering perspective, neutron diffraction is the most attractive prospect as it has superior penetration in many common structural alloys.

This paper presents the results of a study into the measurement of plastic strain in a ferritic steel using neutron diffraction and its potential use in improvement of predictions of structural integrity.

2 Diffraction based strain measurement

The measurement of elastic stress and strain by diffraction methods makes use of Bragg's law which states that diffraction through materials occurs preferentially at certain crystallographic planes, determined by the inter-planar spacing and the wavelength of the incident beam. Neutrons are commonly used for diffraction measurements in engineering materials as they have a typical penetration depth of the order of 50mm in steel, allowing measurements to be made in the interior of specimens.

Bragg's law is generally written as

$$2d_{hkl} \sin\theta = n\lambda, \tag{1}$$

where θ is the diffraction angle, λ the wavelength of the diffracted beam and d_{hkl} is the spacing between the planes of Miller index [hkl]. Strain is determined from the change in spacing of miller index planes, d_{hkl}, between the loaded state and a reference stress free state.

$$\epsilon = \frac{d_{hkl} - d_0}{d_0} = (\theta - \theta_0)\cot\theta. \tag{2}$$

Further details of strain measurement by neutron diffraction can found in a number of published works, e.g. [16, 17], and so will not be entered into here.

2.1 Anistotropy strain

The anisotropy strain method for plastic strain determination is based on measuring the deviation of diffraction peaks from specific crystal planes from their theoretical positions. In a cubic lattice the spacing of a given plane, d_{hkl}, is a function of the unit cell size a

$$d_{hkl} = \frac{a}{\sqrt{h^2 + k^2 + l^2}}. \tag{3}$$

Knowing the material lattice parameter a, equations 1 and 3 can be used to predict the locations of the diffraction peaks for each hkl plane.

However, it has been noted, for example by Ezelio [18] when measuring a Nickel super-alloy and Rogge in stainless steel [19], that the strains measured from differing diffraction peaks began to diverge with increasing deformation. This anisotropy in peak response was further investigated by Daymond and co-workers [20] who modified the standard Rietveld refinement method [21] for diffraction spectra such that the lattice parameter tracks a single peak of Miller index {h00}. The strain from any other peak, ϵ_{hkl}, is then assumed to deviate according to

$$\epsilon_{hkl} = \epsilon_{h00} - \frac{\gamma A_{hkl}}{C} = \epsilon_{h00} - \epsilon_A A_{hkl}, \tag{4}$$

where γ is a fitted anisotropy parameter, C is an instrument constant and A_{hkl} is a measure of the stiffness of individual lattice orientations given by

$$A_{hkl} = \frac{h^2k^2 + k^2l^2 + h^2l^2}{\left(h^2 + k^2 + l^2\right)^2}. \tag{5}$$

This allows definition of an 'anisotropy strain' ϵ_A, where $\epsilon_A = \gamma/C$. It was suggested in [20] that γ and therefore ϵ_A could be partitioned into components due to elastic and plastic strain anisotropy and the measured plastic anisotropy strain ϵ_A^{pl} was found to correlate well with predicted variations in plastic strain. This finding was confirmed by Korsunsky et. al. [22] who used the anisotropy strain method to accurately measure plastic deformation levels in 2024 aluminium.

It is worth noting that the description presented in equation 4 is a simplification of a much more complete description of the complex stress fields introduced by anisotropy of grain alignment. It was observed by Wang et. al. [23] that the more complex spherical harmonics approach was able to reproduce the results of diffraction measurements on a textured austenitic steel. However, the application of the approach of [23] is far from trivial and therefore a more simplistic engineering approximation is employed here.

2.2 Diffraction peak broadening

In a perfectly ordered atomic lattice, under uniform strain, one would expect very sharp diffraction peaks approximating a delta function. In reality, due to inhomogenities inside a typical measurement volume and individual diffraction instrument characteristics, experimental peaks are usually Gaussian in form.

Due to variations in lattice stiffness with orientation, load is not carried evenly across neighbouring material grains. After plastic deformation, this results in the build up of intra-granular residual stresses, meaning two neighbouring grains in the same macroscopic strain field will be experiencing differing levels of local strain. As a result, the diffraction behaviour of each grain will differ slightly, resulting in a broadening of the measured diffraction peak which generally samples multiple material grains. The presence of dislocations may also result in peak broadening, even for measurements based on a single grain, as local regions of tension and compression are created in the surrounding lattice [24]. In fact, data due to Wang and co-workers [25] and Huang et. al. [26] indicates that the majority of the peak broadening effect,

as well as change in peak shape, is due to intra-grannular strains resulting from an increasing dislocation density.

Increasing diffraction peak width was suggested as a method for plastic strain measurement on a welded aluminium bar by Smith [27], although in such cases it is difficult to separate the broadening effects of plastic deformation from those due to local material variations due to the welding process. The peak broadening approach was later used [28] to qualitatively estimate equivalent plastic strain levels in the aluminium sample of [27] as well as in a cracked ferritic steel beam. It was suggested, based on a fit to experimental data, that the relationship between the change in diffraction peak width at half height, $\delta\theta_w$, and the prior plastic strain ϵ_p was given by

$$\delta\theta_w = 0.162\left[1 - \exp\left(-0.3\left|\epsilon_p\right|\right)\right]. \tag{6}$$

It was also noted that the peak broadening was insensitive to the diffraction vector direction, suggesting it is a suitable measure of equivalent plastic strain ϵ_p^e, rather than an approach for determining plastic strain levels in specific directions.

3 Experimental measurements

3.1 Test specimens

In order to investigate the effectiveness of the two discussed methods of plastic strain measurement it was necessary to manufacture suitable test specimens containing well defined plastic strain fields. Tensile test specimens were chosen as calibration specimens for the two techniques. In addition, a number of pre-strained 'blanks' for compact tension (C(T)) type fracture specimens were fabricated in order to compare with the data obtained from the tensile test samples. All samples were manufactured from A533B ferritic steel. This material was chosen as it is part of an ongoing study into the effects of plastic strain on fracture and it is typical of the type of steel commonly used in the power generation industry.

A number of tensile tests were undertaken, according to the ASTM E8 standard, and consistent stress-strain behaviour was recorded in all tests. The tensile test specimens were cylindrical, with diameter 8mm and gauge length 80mm. To pre-strain the C(T) blanks, such that a uniform strain field was created with minimal residual stress, a number of large tensile-type specimens were manufactured. These were preloaded to the desired level of uni-axial plastic strain (1%, 3% and 5%),

determined according to clip gauges fixed to the centre of the specimens, before being cut into sections as illustrated in figure 1.

The specimens used were designed to provide the simplest possible, uni-axial plastic strain field in order to minimise the number of complicating factors when comparing the effectiveness of the two techniques.

3.2 Neutron diffraction measurements

Neutron diffraction measurements were made using the ENGIN-X instrument on the ISIS neutron source at Rutherford Appleton laboratories, U.K. In order to maximise the quality of the diffraction spectra in the thicker pre-strained blanks, while retaining reasonable count times, a gauge volume of $4 \times 4 \times 4\text{mm}^3$ was used for all measurements. A time of flight (TOF) instrument such as ENGIN-X, allowing collection of data from multiple diffraction peaks, was necessary in order to determine the anisotropy strain parameter ϵ_A.

An 'in-situ' tensile test was undertaken on the ENGIN-X instrument in order to record neutron diffraction spectra under varying applied loads. Measurements were taken at increasing levels of plastic strain, with and without applied load in order to separate the elastic and plastic components of peak broadening and anisotropy strain. The results of the in-situ tensile test, along with the data points where diffraction spectra were recorded, are presented in figure 2.

4 Results

The stress-strain response from the tensile test was examined based on the strains recorded from a number of single diffraction peaks in addition to that obtained from Pawley refinement of the entire diffraction spectra. The results are displayed, in comparison to the predicted response based on macroscopic Young's modulus (determined via a strain gauge fixed to the specimen), in figure 3. It can be seen that there exists a significant anisotropy in the response of differing peaks, even in the elastic region. The [200] peak displays strains greater than those predicted from the macroscopic behaviour, as would be expected as it has the lowest stiffness according to equation 5. The strains from each peak then reduce with increasing A_{hkl} with the stiffest response exhibited by the [222] peak with a limiting value of $A_{hkl} = 1/3$.

It can be seen that the Pawley refinement overestimates the macroscopic stiffness which is best represented by the [310] peak response. This is in keeping with the

findings of [20] where the [311] peak was found to provide the best agreement with the macroscopic response in an austenitic steel.

4.1 Anisotropy method results

On examination of the diffraction spectra obtained from both the tensile test (TT) and pre-strained blank (CT) specimens it was decided to limit the data range used to determine anisotropy strains to the three best defined diffraction peaks. In this case these corresponded to the [110], [200] and [211] lattice planes as displayed in figure 4.

The anisotropy strain, ϵ_A, as defined in equation 4 was partitioned into elastic and plastic components, following [20], with the elastic component assumed to vary linearly with the elastic strain in the direction of measurement. This was supported by the data from the TT specimen, displayed in figure 5. Measurements longitudinal and transverse to the loading direction, where elastic strains were tensile and compressive respectively, exhibited ϵ_A values of opposite sign.

The variation of the anisotropy strain under elastic load, ϵ_A^{el}, with the [200] peak strain was found to be well approximated by a linear relationship, as shown in figure 5. The [200] peak strain was selected as it represented the reference peak, corresponding to $A_{hkl} = 0$, used in determination of ϵ_A.

Measurements taken at each unloaded step in the tensile test showed increasing build up of residual elastic strain with increasing plastic deformation, as highlighted in figure 6. It is apparent that in both measured directions the highest magnitude residual strains are present on the [200] peak, with the [310] peak showing the lowest overall level of residual strain in both directions. This again suggest that results based on the [310] plane may be most appropriate for comparison with macroscopic strain predictions such as those from finite element analyses. In both directions the Pawley refinement strain provides a lower bound to the single peak values.

The plastic component of the anisotropy strain, ϵ_A^{pl}, was obtained by subtracting the elastic component, as determined by the linear fit to the [200] peak strain, from the total anisotropy strain. The variation in ϵ_A^{pl} with macroscopic plastic strain, shown in figure 7, shows clear separation between the values obtained in the loaded and unloaded states, suggesting that the plastic anisotropy is not so simply decoupled. It is also apparent, from a comparison between figures 5 and 7 that the 'elastic' component is of much greater magnitude than the plastic component, making accurate determination of ϵ_A^{pl} more difficult. Nonetheless, there is a clear increasing trend between ϵ_A^{pl} and the level of plastic strain, independent of measurement direction,

suggesting that plastic anisotropy may be a reasonable measure of the overall level of plastic deformation.

The results from the pre-strained blanks are plotted in figure 8. As with the tensile test data, the [200] peak strain was used to estimate and remove the 'elastic' component of the anisotropy strain. The results show a similar trend to those made on the TT specimen, although there is a noticeable separation between the values of ϵ_A^{pl} measured in the directions longitudinal and transverse to the pre-strain direction and considerable scatter in the measured value of ϵ_A^{pl} for differing points having experienced the same level of macroscopic plastic strain.

In addition, it is apparent that the magnitude of ϵ_A^{pl} in these specimens is considerably higher than that measured in the TT specimen. This may suggest a geometric component affecting the anisotropy factor, for example measurement path length, or a more complex three dimensional stress-strain state at a granular scale which must be accounted for.

4.2 Peak broadening method results

Traditionally, peak broadening is quantified using the measured peak full width half maximum (FWHM) as this can be easily defined, regardless of the details of the shape of the peak. The peaks recorded in this paper were fitted using a combination of Gaussian, Lorentzian and exponential components to account for peak asymmetry due to the experimental apparatus. The width of a single peak fit is affected only by the Gaussian component, the width of which is in turn a function of the Gaussian parameter σ. As σ is a linear function of the Gaussian peak width and is obtainable directly from the fitting process, it was chosen as an appropriate peak width parameter for this work.

Variation of peak σ, recorded during the tensile test, showed a clear link between the onset of yielding and a dramatic increase in peak width, shown in figure 9. There also appeared to be some weak dependency on elastic strain levels. There was no clear trend in the case of the [310], [222] or [110] peaks, but for the [200] and [211] there appeared to be a linear dependence between the change in peak width, $\Delta\sigma$, and the level of strain in the elastic region. It was found that a linear fit between the absolute elastic strain in the direction of measurement and the change in σ was able to well represent the measured data in the elastic region. Fit was best for the [200] and [211] peaks and, as such, σ values from these two peaks were chosen as representative measures of plastic deformation.

Assuming a linear correlation between the level of elastic strain allowed for a

separation of the elastic and plastic contributions to the peak broadening. Values with and without correction for elastic strain are plotted in figures 10 and 11. It can be seen that removal of the elastic component brings the loaded and unloaded measurements considerably closer together. Following the work of [28], an exponential fit was used to estimate the variation of $\Delta\sigma$ with plastic strain. The best fit equations are included in figures 10 and 11.

Results from the pre-strained blanks showed similar variation between $\Delta\sigma$ and the level of equivalent plastic strain, indicated in figures 12 and 13. The overall magnitudes of the peak breadth increase are significantly larger in the 'blank' specimens than that suggested by the fit to the tensile test data. There is also significant scatter between measurements made in samples with the same level of macroscopic plastic strain.

5 Discussion

From the results obtained it is apparent that both plastic anisotropy strain and diffraction peak broadening are strongly related to levels of macroscopic deformation. It would also appear that there are other influencing factors affecting their variation with the value of macroscopic plastic strain which inhibit accurate calibration and transference of relationships between these parameters from one specimen to another.

Variation of the anisotropy strain was found to be dominated by the elastic strains in the measurement volume, in contrast to the results presented in [20] where the values of ϵ_A^{pl} were of similar magnitude to those obtained for ϵ_A^{el}. Due to the dominance of the elastic anisotropy in this paper, accurate separation of the relatively small plastic component was difficult.

It is also noticeable that, using a simple linear relationship between elastic strain on the [200] peak and ϵ_A^{el}, there is a consistent difference between the values of ϵ_A^{pl} measured with and without external loading (figure 7). This represents a significant problem in terms of using ϵ_A^{pl} as a tool to measure plastic deformation, as the dependence on elastic lattice strain is still apparent.

The results of this paper differ from those in [22] and [20], where ϵ_A^{pl} was seen to vary in a near-linear fashion with plastic strain and was shown to be transferable between geometries. It may be speculated that this difference in response may be due to either the differing crystal structure of the tested materials, as both previous works used FCC materials (austenitic steel and aluminium) in contrast to the BCC

ferritic steel used in the current work, or may be simply due to the difference in anisotropy of plastic and elastic deformation

It can be shown that FCC structure possesses close packed slip planes of Miller index [111]. In the case of a BCC structure there are no close packed planes, resulting in a greater inter-atomic spacing in the slip plane, generally corresponding to [110]. The result is that the Burger's vector $|b|$ for a BCC structure is greater than for the FCC case, equal to $\sqrt{3}a/2$ compared to $a/\sqrt{2}$. This may result in deformation occurring in BCC materials on a smaller number of preferentially aligned slip planes, compared to the FCC case where lower slip energy allows deformation to be more evenly spread across a greater number of planes.

In this case ϵ_A is essentially a measure of disorder in the lattice structure (i.e. deviation from the idealised lattice structure) and likely to be related to dislocation density. Therefore, it may well be that deformation in FCC materials is more easily characterised by this method as dislocation movement is more evenly spread over many slip planes.

Nonetheless this does not explain the considerable increase in ϵ_A^{pl} measured in the extracted blanks compared with the tensile test data. It may be that the deformation at a granular scale in the thicker samples is more disordered that that in the tensile test samples, possibly due to higher constraint levels generating higher stresses transverse to the load direction.

The increase in peak broadening shows only negligible dependence on elastic strain, often within the margin of experimental error which was of the order of $\sigma\pm100$. Despite showing good independence from both elastic strain and measurement direction, the calibrated $\Delta\sigma$ - ϵ_{pl} relationship still underestimated the measured response from the thicker 'blank' samples. This may be a result of the increasing disorientation in the thicker samples or simply the increased measurement path length reducing the accuracy of the measurements. The agreement is, however, significantly better than for the anisotropy method and the tensile test fit provides a reasonable lower bound to the recorded changes in σ in the CT samples. It may be that repeat measurements on a fixed wavelength diffraction instrument, providing more detailed measurements of the shape of a single diffraction peak, may yield better results with this approach than time of flight instruments such as ENGIN-X.

It is also worth noting that plastic strain, in an engineering sense, has questionable relevance at the small scales of interest for diffraction measurements. The two methods used here are based on measurement of increasing inhomogenity of strain experienced by neighbouring grains within the measurement volume. It may well be

that this cannot be simplistically related to the levels of macroscopic deformation without a more rigorous consideration of the deformation at a micro-mechanical scale.

An example may be the existence of Luder's strains which would produce considerable variation in local stresses and strains across local deformation bands. The A533B steel tested has been known to exhibit discontinuous yielding in previous works, e.g. [29], up to around 1% plastic strain. It is notable that the sharpest rise in both ϵ_A^{pl} and $\Delta\sigma$ occurred between 0% and 1% plastic strain in the prestrained blanks so it may be possible that the presence of regions of discontinuous deformation may have contributed to the increase in the scatter and value of both parameters.

It is also important to consider the role of dislocation movement and nucleation during plastic deformation, which may be influenced by a number of microstructural considerations for example grain size, current dislocation population and the local presence of dislocation nucleators such as impurity atoms in the lattice.

6 Conclusions

An investigation was conducted into the ability of diffraction peak broadening and anisotropy of strain determined from differing diffraction peaks to characterise plastic deformation. Variation of parameters with strain in A533B ferritic steel were calibrated from tensile test specimens. The determined relationships between the anisotropy strain ϵ_A^{pl} and change in peak width $\Delta\sigma$ with plastic strain were then used to attempt to measure plastic strain in prestrained blanks for C(T) fracture specimens. The results of the research presented in this paper have produced the following conclusions:

1. The [310] diffraction peak exhibited a minimal effect of elastic or plastic anisotropy in the ferritic steel tested and also provided the closest approximation to the macroscopic stress-strain response. As such it would appear that the [310] peak is an appropriate choice for the determination of macroscopic stresses in such materials.

2. Both the plastic anisotropy strain ϵ_A^{pl} and the peak width broadening parameter $\Delta\sigma$ were found to be correlated with levels of macroscopic strain, although the qualitative variation was found to vary considerably between the sample geometries used in this work.

3. The anisotropy strain due to elastic deformation was found to dominate the overall strain anisotropy response. This is in contrast to previous work on FCC materials (austenitic steels and aluminium) where the elastic and plastic components were of similar magnitude.

4. Plastic strain levels were found to be well correlated with levels of peak broadening, although considerably larger increases in peak width were noted in thicker specimens. It is likely that use of a fixed wavelength instrument to measure a single diffraction peak may reduce the overall scatter in measurements by producing more accurate data on the form of individual peaks.

5. It was noted that many of the problems encountered in this work were not noted in other published works. It is believed that this may be due to the BCC atomic structure of the ferritic steel used in this case, compared to the FCC aluminium and austenitic steels used in other works.

Acknowledgements

The authors would like to thank Dr Sayeed Hossain for his help in conducting the neutron diffraction measurements.

References

[1] A. Kumar, A.J. Wilson, and S.G. Roberts. Quasi-cleavage fracture planes in spherodized a533b steel. *Journal of Microscopy*, 227(3):248–253, 2007.

[2] F.M. Beremin. A local criterion for cleavage fracture of a nuclear pressure vessel steel. *Metall Trans A*, 14A:2277–2287, 1983.

[3] E. Kantidis, B. Marini, and A. Pineau. A criterion for intergranular brittle fracture of a low alloy steel. *Fatigue and Fracture of Engineering Materials and Structures*, 17(6):619–633, 1994.

[4] J.R. Rice and D.M. Tracey. On the ductile enlargement of voids in triaxial stress fields. *Journal of the Mechanics and Physics of Solids*, 17:201–217, 1969.

[5] R.A. Ainsworth, J.K. Sharples, and S.D. Smith. Effects of residual stresses on fracture behaviour - experimental results and assessment methods. *Journal of Strain Analysis*, 35(4):307–316, 2000.

[6] P.A.S. Reed and J.F. Knott. Investigation of the role of residual stresses in the warm prestress (wps) effect. part 1 - experimental. *Fatigue and Fracture of Engineering Materials and Structures*, 19(4):485–500, 1995.

[7] M.R. Daymond, M.W. Johnson, and D.S. Sivia. Analysis of neutron diffraction strain measurement data from a round robin sample. *Journal of Strain Analysis*, 37(1):73–85, 2002.

[8] E. Kingston and D.J. Smith. Residual stress measurements in rolling mill rolls using deep hole drilling technique. *Ironmaking and Steelmaking*, 32(5):379–380, 2005.

[9] G.S. Schajer. Measurement of non-uniform residual stresses using the hole-drilling method. *Journal of Engineering Materials and Technology*, 110:344–349, 1988.

[10] O.M.L. Yahya, F. Borit, R. Piques, and A. Pineau. Statistical modelling of intergranular brittle fracture in a low alloy steel. *Fatigue and Fracture of Engineering Materials and Structures*, 21:1485–1502, 1998.

[11] D.J. Smith. The influence of prior loading on structural integrity. In *Comprehensive Structural integrity*, volume 7. 2003.

[12] S.R. Bordet, A.D. Kartensen, D.M. Knowles, and C.S. Weisner. A new statistical local criterion for cleavage fracture in steel. part 1: model presentation. *Engineering Fracture Mechanics*, 72:435–452, 2005.

[13] L. Xia and C.F. Shih. Ductile crack growth - iii. transition to cleavage fracture incorporating statistics. *Journal of the Mechanics and Physics of Solids*, 44(4):603–639, 1996.

[14] Z. Budrovic, H. Van Swygenhoven, P. Derlet, S. Van Petergem, and B. Schmitt. Plastic deformation with reversible preak broadening in nanocrystalline nickel. *Science*, 304:273–304, 2004.

[15] M. Kamaya, A. Wilkinson, and J. Titchmarsh. Measurmement of plastic strain of polycrystalline material by electron backscatter diffraction. *Nuclear Engineering and Design*, 235:713–725, 2005.

[16] G.A. Webster and R.C. Wimpory. Non-destructive measurement of residual stress by neutron diffraction. *Journal of Materials Processing Technology*, 117:395–399, 2001.

[17] M.E. Fitzpatrick and A. Lodini. *Analysis of Residual Stress by Diffraction using Neutron and Synchrotron Radiation*. Taylor and Francis, New York, 2003.

[18] A.N. Ezelio, G.A. Webster, P.J. Webster, and X. Wang. Characterisation of elastic and plastic deformation in a nickel superalloy using pulsed neutrons. *Physica B*, 180:1044–1046, 1992.

[19] R.B. Rogge, P.R. Dawson, and D. Boyce. Neutron diffraction measurment of the evolution of strain for non-uniform plastic deformation. *Applied Physics*, A74:1725–1727, 2002.

[20] M.R. Daymond, M.A.M. Bourke, R.B. Von Dreele, B. Clausen, and T. Lorentzen. Use of rietveld refinement for elastic macrostrain determination and for evaluation of plastic strain history from diffraction spectra. *Journal of Applied Physics*, 82(4):1554–1562, 1997.

[21] H.M. Rietveld. A profile refinement method for nuclear and magnetic structures. *Journal of Applied Crystallography*, 2:65–71, 1969.

[22] A.M Korsunsky, M.R. Daymond, and K.E. James. The correlation between plastic strain and anisotropy strain in aluminium alloy polycrystals. *Materials Science and Engineering*, A334:41–48, 2002.

[23] Y. D.Wang, R. Lin Peng, and R. L. McGreevy. A novel method for constructing the mean field of grain-orientation-dependent residual stress. *Philosophical Magazine Letters*, 81(3), 2001.

[24] W.G. Moffatt, G.W. Pearsall, and J. Wulff. *The Structure and Properties of Materials, Vol. 1, Structure*. John Wiley and Sons, New York, 1964.

[25] X.-L. Wang, Y.D. Wang, A.D. Stoica, D.J. Horton, H. Tianc, P.K. Liawc, H. Chooc, J.W. Richardson, and E. Maxey. Inter- and intragranular stresses in cyclically-deformed 316 stainless steel. *Materials Science and Engineering A*, 399:114–119, 2005.

[26] E-Wen Huang, Rozaliya, I. Barabash, Yandong Wang, Bjrn Clausen, Li Li, Peter K. Liaw, Gene E. Ice, Yang Ren, Hahn Choo, Lee M. Pike, and Dwaine L. Klarstrom. Plastic behavior of a nickel-based alloy under monotonic-tension and low-cycle-fatigue loadingl. *International Journal of Plasticity*, 24:1440–1456, 2008.

[27] D.J. Smith, R.H. Leggatt, G.A. Webster, H.J. Macgillivray, P.J. Webster, and G. Mills. Neutron diffraction measurments of residual stress and plastic deformation in an aluminium alloy weld. *Journal of Strain Analysis*, 23(4):201–211, 1988.

[28] D.J. Smith and G.A. Webster. The measurement of prior plastic deformation in metallic alloys using the neutron diffraction technique. *Journal of Strain Analysis*, 32(1):37–46, 1997.

[29] A. Mirzaee-Sisan. *The influence of prior thermal and mechanical load on fracture*. Ph.d thesis, University of Bristol, 2005.

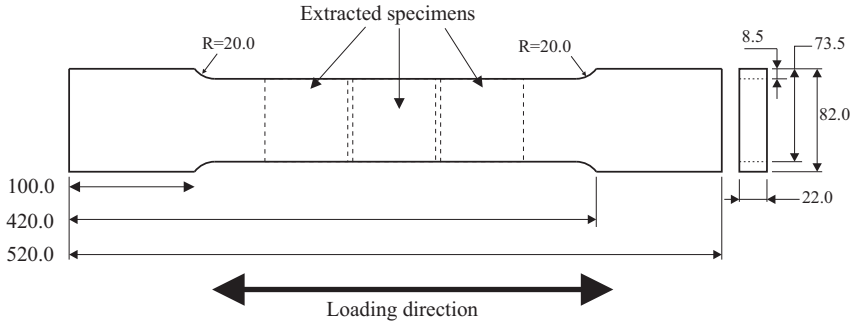

Figure 1: Large tensile specimens, used to generate uniform plastic strain in extracted 'blanks'. Dimensions in mm

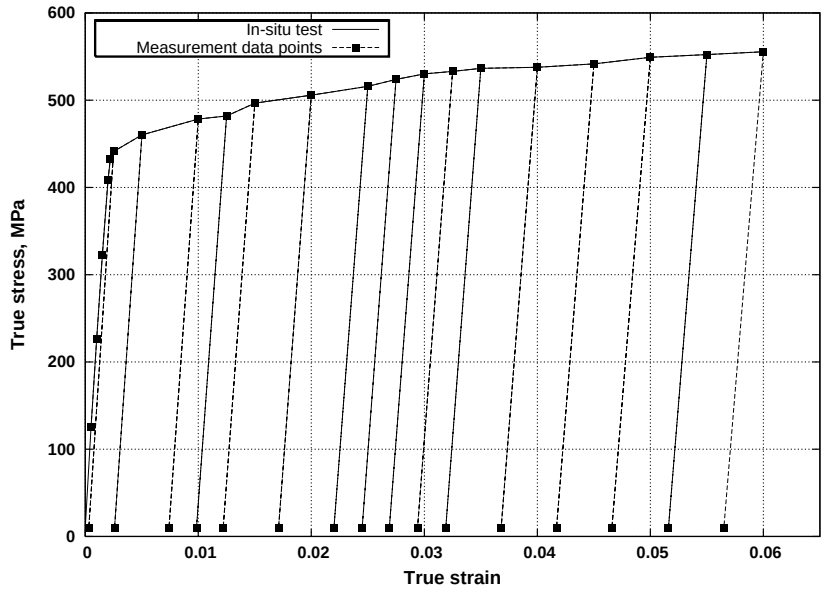

Figure 2: Material stress-strain response from in-situ tensile testing showing points where calibration diffraction measurements were undertaken

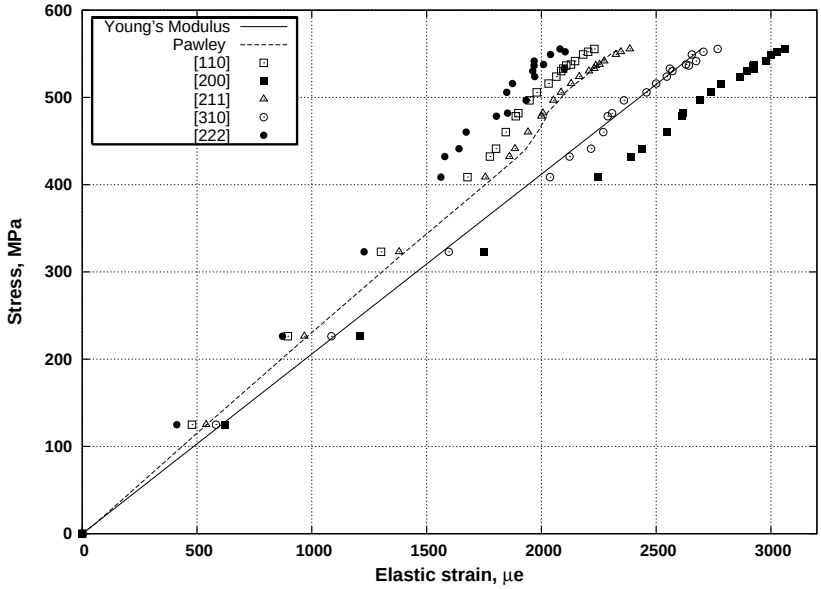

Figure 3: Strain measurements from in-situ tensile test based on full Pawley refinement of the full diffraction spectra and analysis of individual peaks

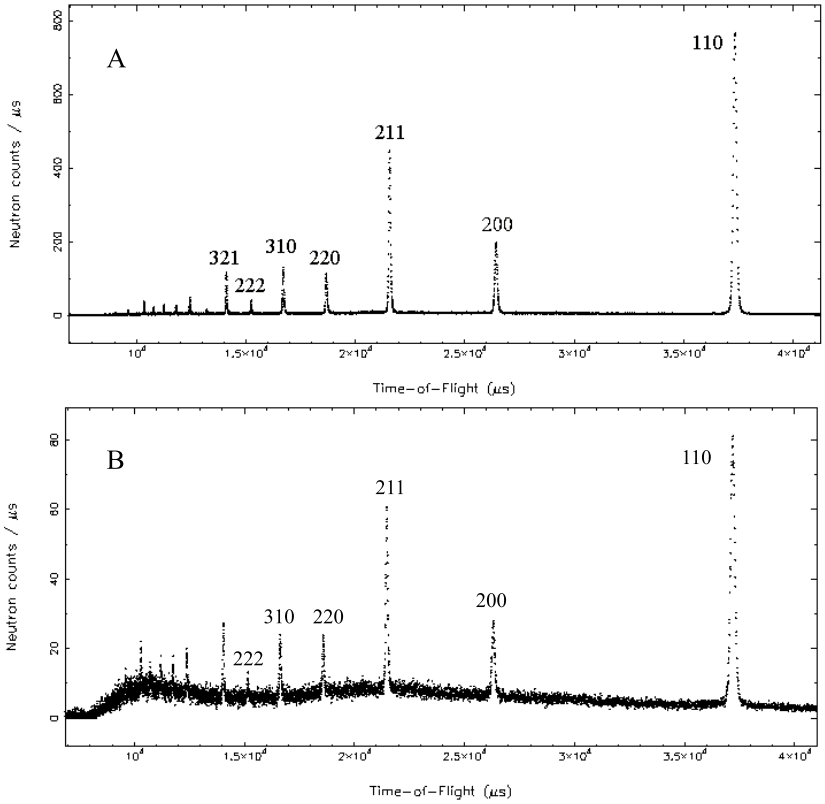

Figure 4: Diffraction spectra recorded from A) Tensile test specimens and B) extracted prestrained blanks

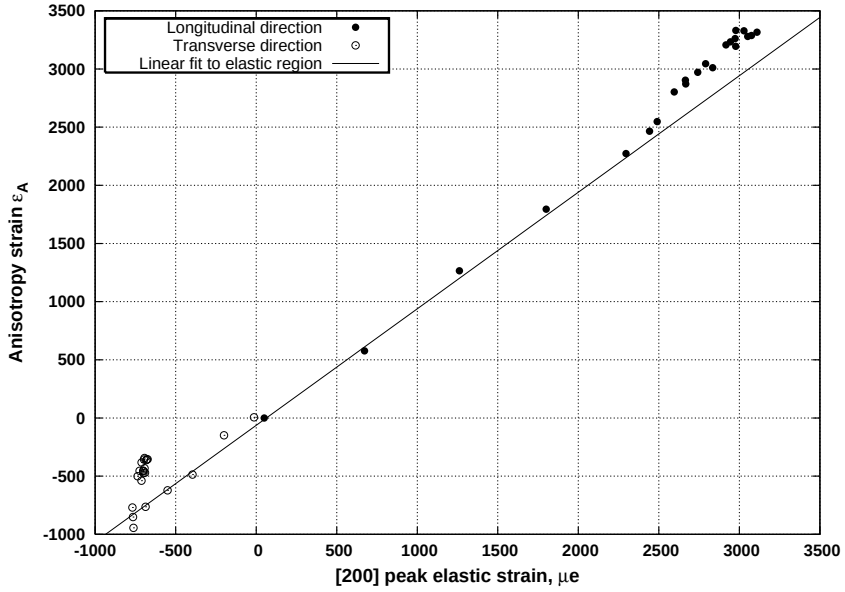

Figure 5: Evolution of the anisotropy strain, ϵ_A, measured in the tensile test specimen in directions longitudinal and transverse to the loading axis

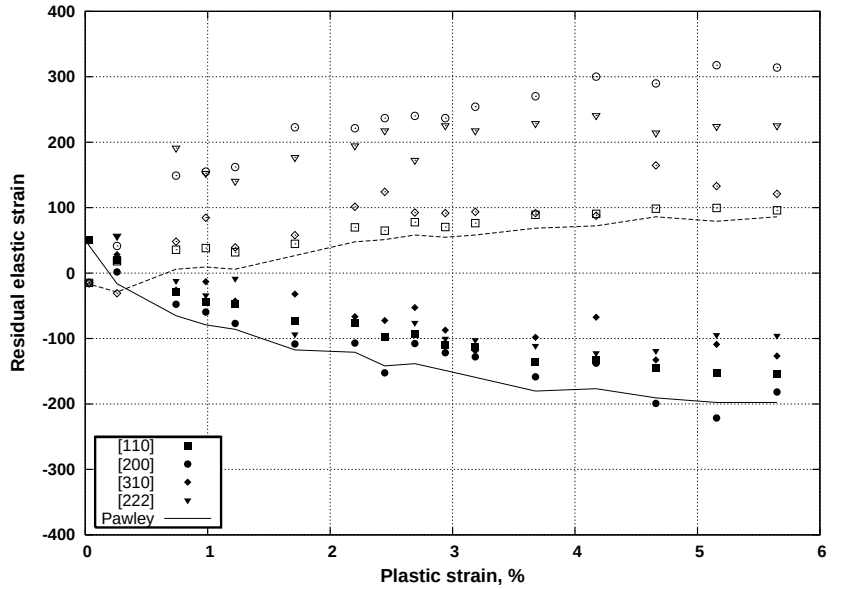

Figure 6: Residual strains, based on single diffraction peaks and Pawley refinement, measured in the tensile test specimen upon unloading to 10MPa. Filled symbols denote longitudinal strains, open symbols correspond to transverse strains

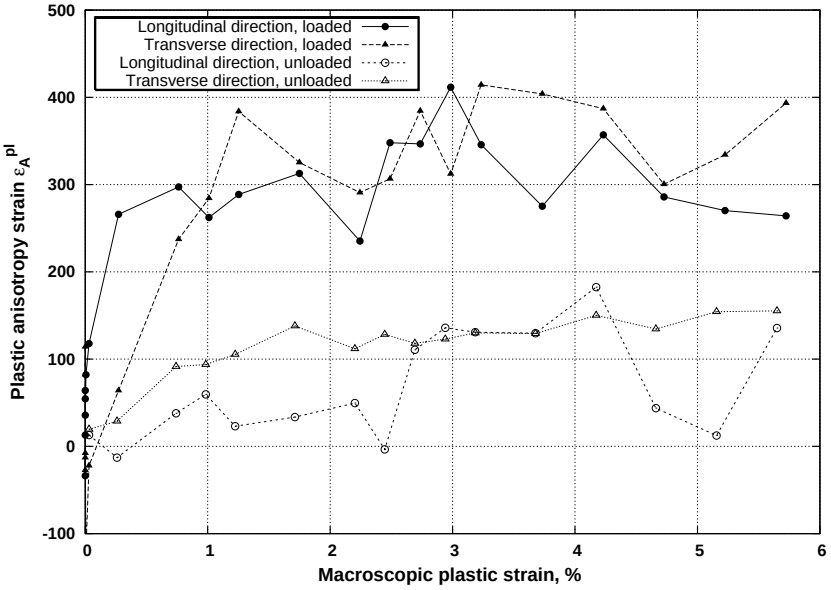

Figure 7: Plastic anisotropy strain, ϵ_A^{pl}, measured in the tensile test specimen in loaded and unloaded states, in directions longitudinal and transverse to the loading axis

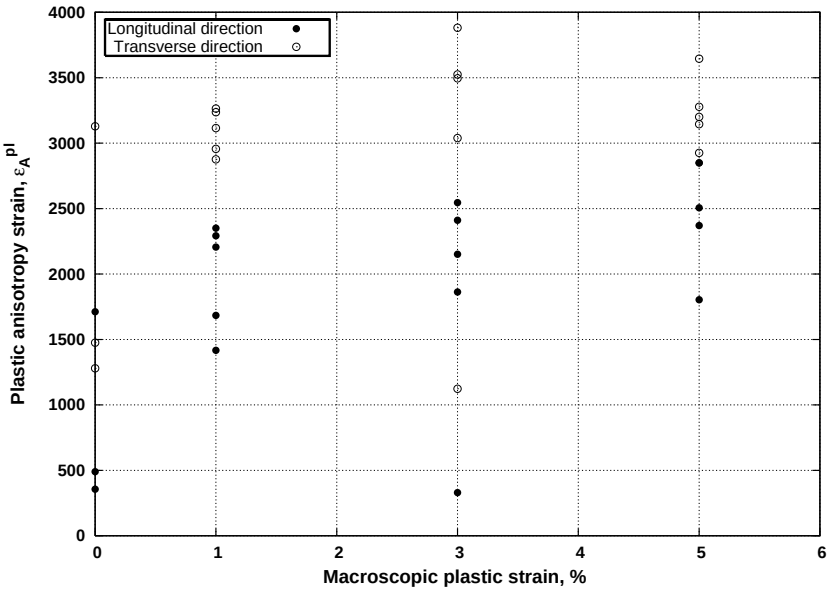

Figure 8: Plastic anisotropy strain, ϵ_A^{pl}, measured in the extracted C(T) blanks, in directions longitudinal and transverse to the loading axis

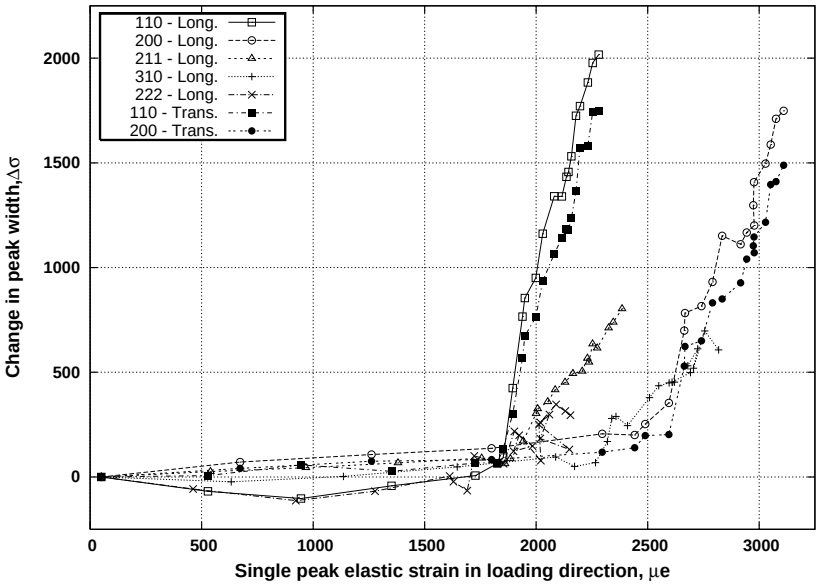

Figure 9: Variation in peak σ component as a function of peak strain, as recorded during the in-situ tensile test

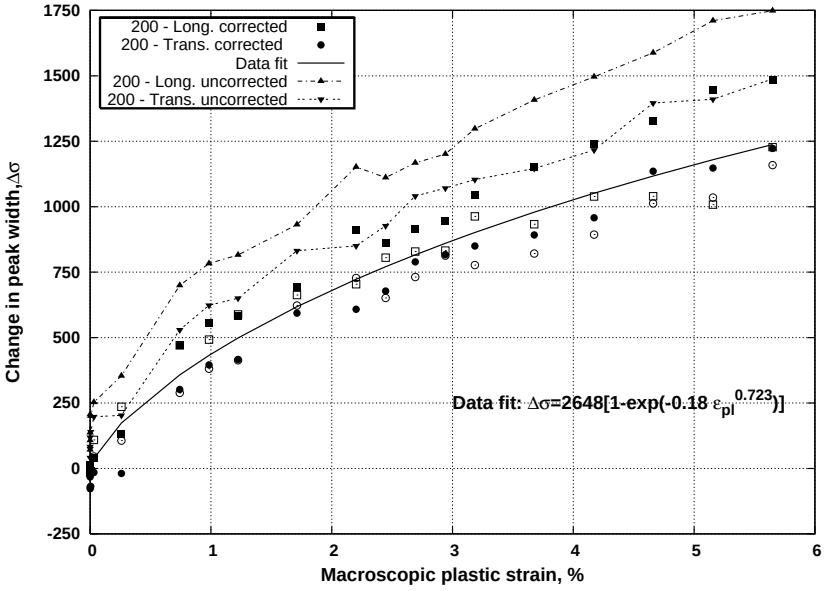

Figure 10: Variation in [200] peak σ component as a function of macroscopic plastic strain, as recorded during the in-situ tensile test. Open and closed symbols represent the loaded and unloaded states for each plastic strain level

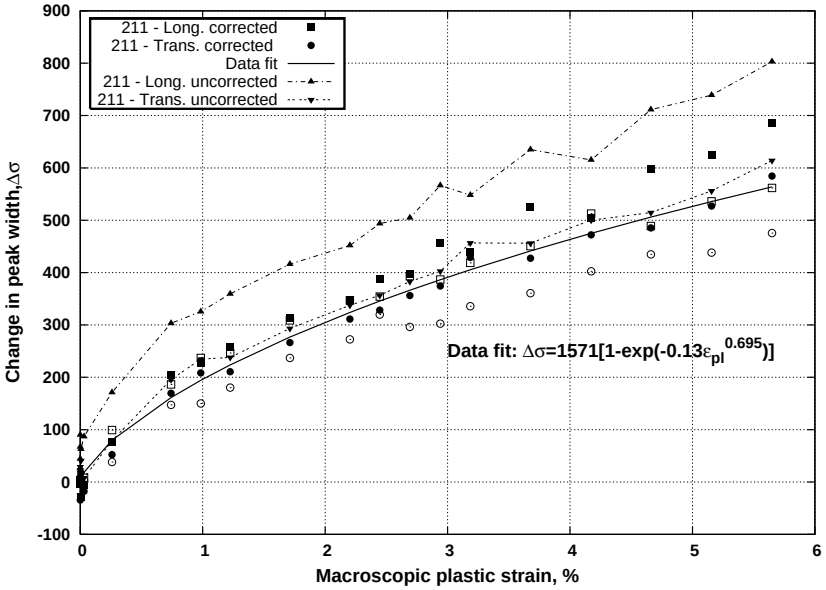

Figure 11: Variation in [211] peak σ component as a function of macroscopic plastic strain, as recorded during the in-situ tensile test. Open and closed symbols represent the loaded and unloaded states for each plastic strain level

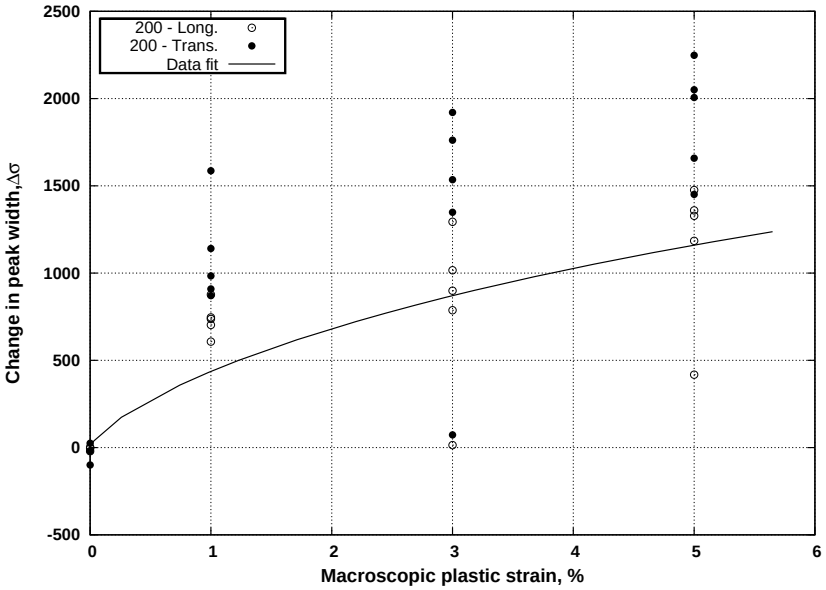

Figure 12: Variation in [200] peak σ component as a function of macroscopic plastic strain, as recorded in extracted prestrained blanks, compared with analytical broadening function as fitted to tensile test data

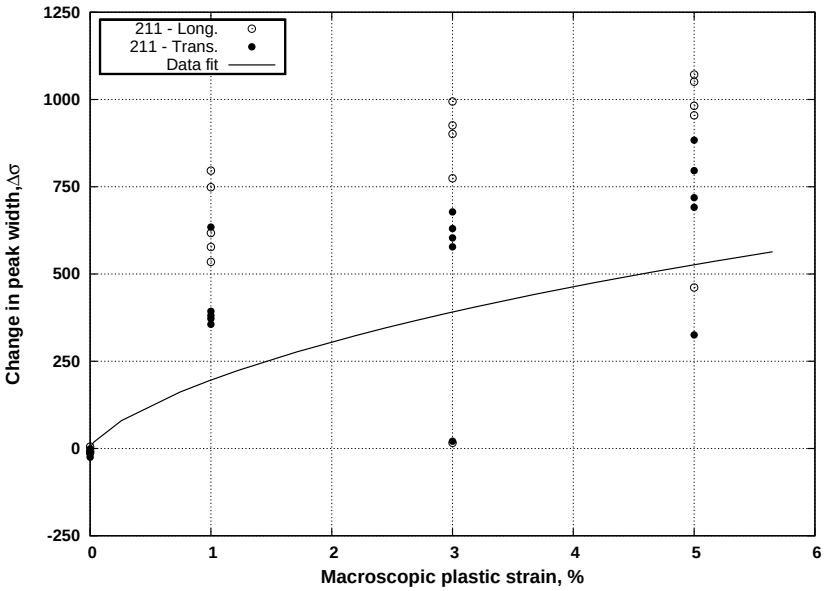

Figure 13: Variation in [211] peak σ component as a function of macroscopic plastic strain, as recorded in extracted prestrained blanks, compared with analytical broadening function as fitted to tensile test data